Sensors and Materials, Vol. 38, No. 4 (2026) 2169–2185
MYU Tokyo

S & M 4429

One-time-varying Sliding Mode Control and Adaptive-type Control of State Synchronization for Unified Chaotic Systems

Chi-Hsin Yang*

School of Intelligent Manufacture and Electronic Engineering,
Guangzhou Institute of Science and Technology, Guangzhou City 510540, Guangdong Province, China

(Received November 18, 2025; accepted April 21, 2026)

Keywords: time-varying sliding mode control (SMC), adaptive time-varying SMC, state synchronization, unified chaotic system, antipodal chaos shift keying (ACSK)

In this paper, a time-varying sliding mode control (SMC) strategy and an adaptive enhancement of SMC to achieve state synchronization in unified chaotic systems are presented. A dedicated sliding mode function and its corresponding control law are developed to drive the synchronization error states onto the sliding surface and sustain them there. Once on the surface, complete state synchronization is achieved as the first two error states converge to zero within a finite time, while the third error state asymptotically approaches zero through exponential decay. However, the initial control design exhibits notable chattering in the control input, which is mitigated by introducing an adaptive time-varying SMC scheme that effectively suppresses such a chattering effect. The proposed adaptive approach employs online-updated state feedback gains that adjust in real time in accordance with the designed adaptation laws without requiring prior knowledge of system nonlinearities, lumped uncertainties, or external disturbances. The stability of the closed-loop error system is rigorously proven using Lyapunov stability theory, and numerical simulations are conducted to validate the effectiveness and robustness of the proposed control schemes. The proposed control algorithm has future potential in signal transmission and sensing, such as antipodal chaos shift keying (ACSK) in a spread-spectrum chaotic communication system. The pending problems lie in developing a functional ACSK system by applying the proposed algorithm and facing the limitations such as the degradation of noise mitigation efficacy and the expenses of hardware implementation. Overcoming these points will be future works of this study.

1. Introduction

Even slight modifications to the original conditions can produce exponentially different results because chaotic systems are extremely sensitive to them. They can be found in many areas of both natural and artificial systems, including electronic circuits,[1–3] mechanical systems,[4–8] and ecosystems.[9,10] Furthermore, Stenflo reported his work on chaotic systems in meteorology.[11] The intricate dynamical features of chaotic systems offer both opportunities and

*Corresponding author: e-mail: 2576805728@qq.com
https://doi.org/10.18494/SAM6064

ISSN 0914-4935
https://myukk.org/

problems from the standpoint of engineering applications, making the theoretical and practical significance of comprehending and managing chaotic behavior noteworthy. Consequently, Pecora and Carroll introduced synchronization between two chaotic systems.[12] This research topic has garnered a lot of attention since they proposed the idea of master–slave chaotic synchronization. Chaotic synchronization has several significant uses, including secure communication[13,14] and encryption.[15–17]

The aim of state synchronization is to make every state variable in the master chaotic system monitor every state for a slave system correspondingly. In previous works, Yang[18,19] and Chaudhary *et al*.[20] investigated the synchronization control of chaotic systems by nonlinear control technologies. Real chaotic systems frequently include particular features, such as different types of disturbances and uncertainties, and the chaotic phenomenon is highly sensitive to changes in initial value and parameters. This topic is still a significant and challenging problem that must be solved immediately since several engineering applications still struggle to establish the synchronization control of uncertain chaotic systems with unknown parameters utilizing control techniques. Researchers have suggested and validated a number of control methods to achieve this aim, including finite-time control,[21–24] sliding mode variable structure control,[25,26] the dynamic surface approach,[27] robust control,[28] and adaptive feedback synchronization control.[29–34] Theoretical research is intensifying, and control approaches are maturing. Thus, achieving the synchronization of chaotic systems with a minimal structure, limited control, and finite time will be the focus of chaotic-synchronization research.

Studying the issue of state synchronization between two unified chaotic systems is motivated by the aforementioned studies. The slave chaotic system is taken into consideration in the control problem by being connected to a single input controller when lumped system uncertainties and outside disturbances are present. Lü and Chen developed the unified chaotic system,[35] which is given by

$$\begin{aligned} \dot{x}_m(t) &= (25h+10)(y_m(t)-x_m(t)), \\ \dot{y}_m(t) &= (28-35h)x_m(t)+(29h-1)y_m(t)-x_m(t)z_m(t), \\ \dot{z}_m(t) &= x_m(t)y_m(t)-(8+h)z_m(t)/3, \end{aligned} \tag{1}$$

where $x_m(t)$, $y_m(t)$, and $z_m(t)$ represent the state variables and $h \in [0,1]$ is the system parameter. The canonical Lorenz system[36] and the Chen system[37] are respectively the two extremes for $h = 0$ and $h = 0.8$. Additionally, as a particular instance of the system in Eq. (1), the Lü system[35] occurs when $h = 1$. Note that the resulting system is always chaotic as the parameter h fluctuates between 0 and 1. Celikovsky and Chen thoroughly examined and discussed the unified chaotic system's nonlinear dynamic properties.[38]

By appropriately choosing the resistors R_i, $i = 1, 2, ..., 22$ and the capacitors C_i, $i = 1,2,3$ and adjusting the switches S_i, $i = 1,2$, the electronic circuit implementation depicted in Fig. 1 may accurately depict the dynamics of the three chaotic systems described by Eq. (1). By turning S_1 off and S_2 on, the electronic circuit transforms into the Lorenz system. Otherwise, the electronic circuit functions like the Chen system when S_1 is turned on and S_2 is turned off. The dynamics of the Lü system are achieved when both S_i, $i = 1,2$, are turned off. The output voltage of this

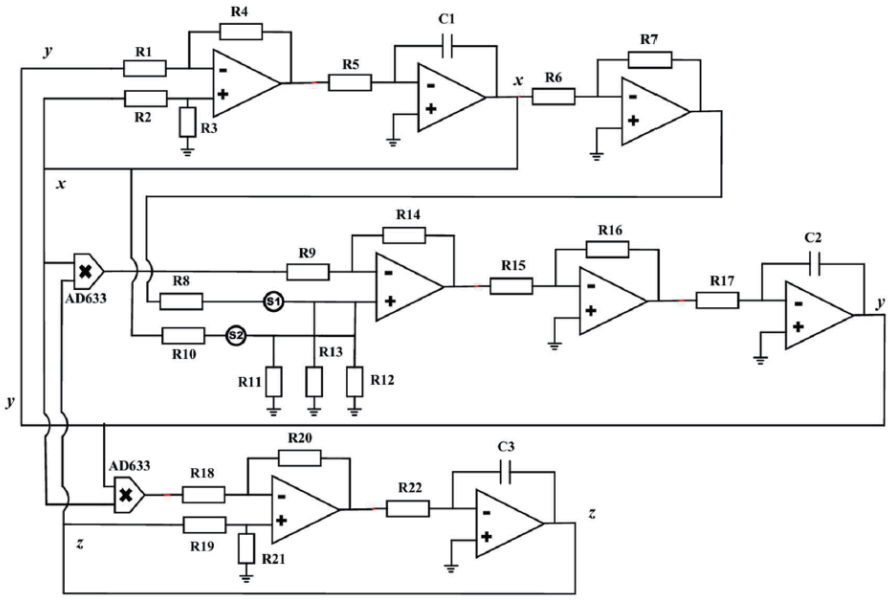

Fig. 1. Circuit implementation of the unified chaotic system.

circuit can be accurately determined by incorporating appropriately configured voltage sensing devices. Furthermore, the evolution of Lyapunov exponents as a function of the unified chaotic system parameter h is presented in Fig. 2. It is evident that the maximum Lyapunov exponent λ_1 remains positive and $\sum_{i=1}^{3}\lambda_i < 0$, which indicates the presence of chaotic dynamics in the system.

In addressing the control challenges of the unified chaotic system, Yassen developed a linear feedback control method and constructed an adaptive controller to stabilize the system around its equilibrium.[39] To mitigate chaotic oscillations, Takhi *et al.* employed sliding mode control (SMC) by leveraging the inherent robustness of the system.[40] With respect to state synchronization, Wei *et al.* realized an adaptive control scheme for state synchronization between master and slave chaotic systems.[41] Furthermore, Wang *et al.* examined the finite-time synchronization for the same systems.[42]

In this study, the proposed control algorithm, which incorporates the advancements in state synchronization for the unified chaotic systems, has a wide range of applications to encryption techniques in the field of secure communication and voice encryption.[43,44] The algorithm serves as a key technical cornerstone for advancing research and innovation in secure signal transmission and sensing. A concrete application example of the proposed algorithm is presented. Antipodal chaos shift keying (ACSK) based on chaotic synchronization[45] is a demodulation technique employed in spread-spectrum chaotic communication systems. Figure 3 illustrates the block diagram of the implemented ACSK system, which utilizes chaotic synchronization for demodulation.

The ACSK system consists of three chaotic generators based on the unified chaotic system in Eq. (1). One master chaotic generator is located at the transmitting end, while two slave chaotic generators with the control algorithm proposed in this study are located at the receiving end. The following three main steps can complete the spread-spectrum chaotic communication of the communicated signal.[45]

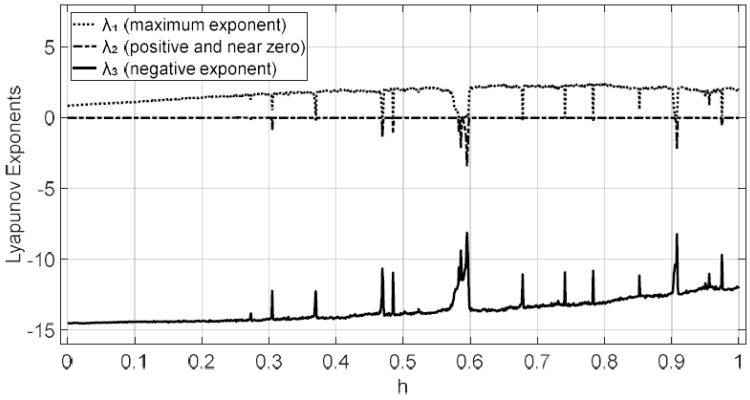

Fig. 2. Lyapunov exponents of the unified chaotic system for $h \in [0,1]$.

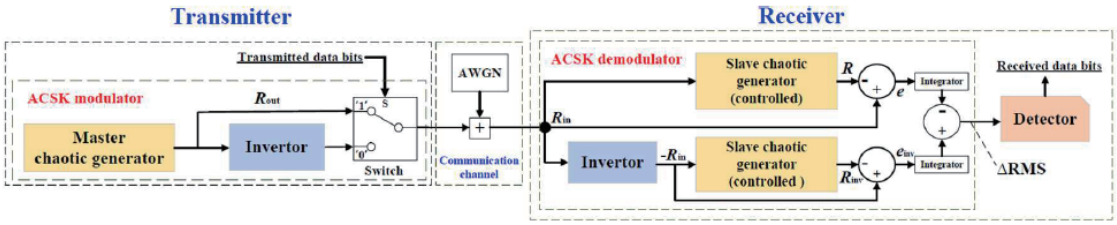

Fig. 3. (Color online) Chaotic-synchronization-based ACSK.

(1) Within the ACSK modulator, the output chaotic signal R_{out} is produced by dynamically selecting between the unaltered and phase-reversed versions of the chaotic waveform, which is governed by the transmitted data bits (0 or 1) via a controlled switch. The waveform variation of R_{out} is analytically represented as a weighted sum of the state variables characterized by the unified chaotic system in Eq. (1). For a transmitted "0", the underlying chaotic trajectory is subjected to sign reversal, and for a "1", it is passed through unchanged. As a result, transmitted data bits are seamlessly encoded onto the chaotic spread signal R_{out}, supporting robust and synchronized chaotic communication. Consequently, in the communication channel, additive white Gaussian noise (AWGN) is applied to the spread signal R_{out} and its inverted signal.

(2) In the receiver's ACSK demodulator, two chaotic slave generators with controls, provided in this study, are used to synchronize with the input signal R_{in}, one for the direct and one for the inverted chaotic signal $-R_{in}$. Using the signal R_{in} as an input for both slave chaotic generators, it is possible to restore the output signal R, which is synchronized and similar to the signal R_{out} from the master chaotic generator, in the demodulator.

(3) Synchronization is quantified through two error terms, $e = R_{in} - R$ and $e_{inv} = -R_{in} - R_{inv}$, with R and R_{inv} being the outputs of the respective slave chaotic oscillators. Each error waveform is first integrated across one symbol period. From the resulting integrated waveforms, root-mean-squared (RMS) amplitudes are extracted, and ΔRMS is then obtained as the magnitude

of their difference. In the detection scheme in the detector, ΔRMS functions as the discriminating metric. Transmitted data bits are recovered by identifying the received data bits that yield the minimized ΔRMS, where this quantity is estimated via temporal averaging over the entire transmitted-data-bits interval.

In this study, a time-varying SMC approach and the control scheme augmented with an adaptive mechanism are proposed to achieve state synchronization in unified chaotic systems. The main novelty and contribution of this study are summarized as follows.

(1) A time-varying sliding mode function $\sigma(t)$ is introduced, and a corresponding control law is designed to drive $\sigma(t)$ to the sliding surface $\sigma(t) = 0$ and maintain it there, forming the foundation of the proposed control scheme.
(2) It is further demonstrated that the first two state variables, $e_1(t)$ and $e_2(t)$, of the synchronization-error dynamical system reach zero in finite time after the condition $\sigma(t) = 0$ is met, while the third state variable, $e_3(t)$, decays exponentially toward zero. This guarantees full state-synchronization between the unified chaotic systems. Then, a thorough theoretical explanation is included to support these dynamic tendencies.
(3) To address the pronounced chattering effect exhibited by the control input in the original design from step (1), an improved adaptive type of the time-varying SMC scheme is developed on the basis of the same sliding mode function $\sigma(t)$, significantly reducing undesirable input-chattering effects.
(4) Simulation studies verify that both control strategies effectively accomplish the state synchronization goal for the pair of unified chaotic systems under consideration.
(5) The developed algorithm has future potential for application to encryption techniques in signal transmission and sensing, such as a chaotic-synchronization-based ACSK system.

One major pending problem involves translating the proposed control algorithm into a fully functional chaotic-synchronization-based ACSK system. While theoretically promising, the algorithm still faces limitations. For example, the developed system's noise mitigation efficacy may possibly degrade notably in real-world channel environments, and the embedding of the nonlinear control logic into physical hardware remains hindered by substantial design complexity and elevated implementation expenses. Overcoming these hurdles is central to our subsequent investigative efforts.

In Sect. 2, the state synchronization control problem between two unified chaotic systems is formulated and described. In Sect. 3, the time-varying SMC and an enhanced adaptive-type control are deduced. Sufficient conditions from the perspective of the Lyapunov stable theorem are also provided. Numerical simulations are used to test the current scheme's capacity in Sect. 4, and remarks are given. Lastly, Sect. 5 concludes with some findings.

2. Descriptions of Control Problem

In this work, the issue of state synchronization control between two identical unified chaotic systems, described by Eq. (1), is examined. The master system, which functions autonomously without external control input, serves as the reference model. In contrast, the slave system receives a single control signal and is affected by the combination of system uncertainties and

external disturbances. To facilitate a clear and systematic analysis, the dynamics of the master system are represented by Eq. (1), providing a benchmark for the design and implementation of the slave system's control strategy. The slave system is defined by

$$\begin{aligned}
\dot{x}_s(t) &= (25h+10)(y_s(t)-x_s(t)),\\
\dot{y}_s(t) &= (28-35h)x_s(t)+(29h-1)y_s(t)-x_s(t)z_s(t)+\Delta f(t)+\Delta(t)+\mu(t),\\
\dot{z}_s(t) &= x_s(t)y_s(t)-(8+h)z_s(t)/3,
\end{aligned} \tag{2}$$

where $x_S(t)$, $y_S(t)$, and $z_S(t)$ denote the state variables, $\Delta f(t) \in R$ represents the bounded lumped system uncertainty satisfying $0 < \left|\Delta f\right| < \Omega_f$, $\Delta(t) \in R$ is the external disturbance satisfying $0 < \left|\Delta(t)\right| < \Omega_d$, and $\mu(t) \in R$ denotes the control input.

The objective of the control problem is to design a single-input controller in the system described by Eq. (2) such that state synchronization between systems of Eqs. (1) and (2) can be achieved, without prior knowledge of the specific lumped system uncertainties or external disturbances. The state synchronization error between Eqs. (1) and (2) is defined as

$$e_1(t) = x_s(t) - x_m(t),\ e_2(t) = y_s(t) - y_m(t),\ e_3(t) = z_s(t) - z_m(t). \tag{3}$$

After deducting Eq. (1) from Eq. (2), the error-state dynamical system can be represented as the time derivatives of Eq. (3).

$$\begin{aligned}
\dot{e}_1(t) &= (25h+10)(e_2(t)-e_1(t))\\
\dot{e}_2(t) &= (28-35h)e_1(t)+(29h-1)e_2(t)+\delta(t)+\Delta f(t)+\Delta(t)+\mu(t)\\
\dot{e}_3(t) &= x_s(t)e_2(t)+y_m(t)e_1(t)-(8+h)e_3(t)/3
\end{aligned} \tag{4}$$

Here, $\delta(t) = -x_s(t)e_3(t) - z_m(t)e_1(t)$ is the nonlinear function. It is a reasonable assumption that $\delta(t)$ is bounded with $|\delta(t)| < D$ since the chaotic system always displays globally bounded state trajectories. Additionally, the control input is bounded $\left|\mu(t)\right| \le u_{max}$ and it is expected that $\left|\delta(t)+\Delta f(t)+\Delta(t)\right| < M < u_{max}$.

It is evident that the control problem of state synchronization between systems of Eqs. (1) and (2) is mathematically analogous to the problem of using a suitable control scheme $\mu(t)$ to stabilize the error states of the dynamical system of Eq. (4). Therefore, determining the appropriate control scheme $\mu(t)$ that will cause all error states of the dynamical system to converge to zeros, or $\lim_{t\to\infty} e_i(t) \to 0, i = 1,2,3,$ for any beginning state of the system of Eq. (4) is the aim of the current challenge.

3. Design of Control Schemes

SMC is a robust nonlinear control method tolerant to system variations and external disturbances. It employs a time-invariant sliding surface in the state space, then state trajectories are driven onto that surface and then constrained to evolve along it until asymptotically reaching

the origin or desired equilibrium. Once on the surface, the reduced-order dynamics depend solely on its geometry, rendering the closed-loop response insensitive to certain modeling errors and exogenous perturbations. However, conventional SMC suffers from chattering due to discontinuous control switching, which is typically mitigated via smoothing or boundary-layer approximations. In contrast to fixed-sliding-surface designs, our proposed design is an adaptive, time-varying sliding surface tailored to the nonlinear system in Eq. (4), explicitly accommodating both bounded external disturbances and system uncertainties.

There are two primary steps in the suggested strategy. The first step is choosing a suitable time-varying sliding mode function $\sigma(t)$ for the intended sliding motion. Second, any trajectory of $\sigma(t)$ in phase space can be brought to and maintained on the sliding surface, $\sigma(t) = 0$, by designing a robust controller. The synchronous error states will converge to zeros on the sliding surface in accordance with the sliding mode's convergent feature. It creates the illusion that the master system can be synchronized with the slave system. In this section, two control schemes are performed, that is, the time-varying SMC and the adaptive type enhancement.

The time-varying sliding mode function is chosen by

$$\sigma(t) = e_2(t) - e_1(t) + c(t)\left[e_1(t)\right]^{q/p}, \tag{5}$$

where $0 < q/p < 1$ and $p > q > 0$ are positive and odd integers. The time function $c(t)$ is defined by

$$c(t) = \begin{cases} nt, & 0 \le t < t_0 \\ nt_0, & t \ge t_0 \end{cases} \tag{6}$$

with $n = (u_{\max} - M)\Big/\left|e_1(0)\right|^{q/p}$. $e_1(0)$ is the initial value of $e_1(t)$. $t_0 > 0$ is a specific value of time, named the switching time, and will be defined later.

In the sequel, by considering that the control input is bounded as $\left|\mu(t)\right| \le u_{max}$ and reasonably assuming that $\left|\delta(t) + \Delta f(t) + \Delta(t)\right| < M < u_{max}$, the time-varying SMC scheme for achieving synchronization is proposed in Theorem 1.

Theorem 1.

If the control input $\mu(t)$ in Eq. (2) is introduced as

$$\begin{aligned} \mu(t) = &-(18 - 60h)e_1(t) - (9 + 54h)e_2(t) - \dot{c}(t)\left[e_1(t)\right]^{q/p} \\ &- c(t)(\alpha q / p)\left[e_2(t) - e_1(t)\right]\left[e_1(t)\right]^{q/p-1} - M\,\mathrm{sign}(\sigma(t)), \end{aligned} \tag{7}$$

where $\alpha = 25h + 10$ and sign(·) denotes the sign function, then the states of the error dynamical system (4) will asymptotically approach and stay on the sliding mode surface $\sigma(t) = 0$ defined by Eq. (5).

Proof. The scale Lyapunov function is selected as $\Psi_1(t) = 0.5\sigma^2(t) \ge 0$. Taking the time derivative of the function $\Psi_1(t)$ along with the solutions of the error-state dynamical system in Eq. (4), the

selection of the time-varying sliding mode function in Eq. (5), and the control input in Eq. (7), we obtain

$$\begin{aligned}\dot{\Psi}_1(t)=\sigma(t)\dot{\sigma}(t) &= \sigma(t)\Big[\dot{e}_2(t)-\dot{e}_1(t)+\dot{c}(t)\big[e_1(t)\big]^{q/p}+c(t)(q/p)\big[e_1(t)\big]^{(q/p)-1}\dot{e}_1(t)\Big]\\ &\quad+\sigma(t)\big[\delta(t)+\Delta f(t)+\Delta(t)+\mu(t)\big]\\ &= \sigma(t)\big[\delta(t)+\Delta f(t)+\Delta(t)-M\,\mathrm{sign}(\sigma(t))\big]\\ &\le \big|\delta(t)+\Delta f(t)+\Delta(t)\big|\big|\sigma(t)\big|-M\big|\sigma(t)\big| = -\Big(M-\big|\delta(t)+\Delta f(t)+\Delta(t)\big|\Big)\big|\sigma(t)\big|<0.\end{aligned}$$

Therefore, the condition of $\dot{\Psi}_1(t)<0$ is satisfied. The time-varying sliding mode function $\sigma(t)$ can asymptotically reach and stay at $\sigma(t) = 0$. This completes the proof of Theorem 1.

Theorem 2.

When the time-varying sliding mode function in Eq. (5) is maintained at $\sigma(t) = 0$ by applying the control $\mu(t)$ in Eq. (7), then the error states $e_1(t)$, $e_2(t)$ of the dynamical system in Eq. (4) converge to and remain at zero at the finite time $t = t_f$. Furthermore, the error state $e_3(t)$ is stabilized exponentially after $t = t_f$. The finite time $t = t_f$ is given by

$$t_f=\left(\frac{1}{1-(q/p)}\sqrt{\frac{q}{\alpha p}}+\frac{1}{2}\sqrt{\frac{p}{\alpha q}}\right)\sqrt{\frac{|e_1(0)|}{u_{\max}-M}}. \tag{8}$$

Proof.

The proof of this theorem is composed of two parts. First, the stability of the error states is established. Subsequently, the finite time $t = t_f$ in Eq. (8) and the switching time $t_0 > 0$ are derived.

(1) The solution of the error state $e_1(t)$ is derived. For $\sigma(t) = 0$ in Eq. (5),

$$e_2(t)-e_1(t)=c(t)\big[e_1(t)\big]^{q/p}. \tag{9}$$

The differential equation of $e_1(t)$ becomes

$$\dot{e}_1(t)=\alpha\big[e_2(t)-e_1(t)\big]=-\alpha c(t)\big[e_1(t)\big]^{q/p}. \tag{10}$$

On the basis of the definition of the time function $c(t)$ provided in Eq. (6), the solution for $e_1(t)$ is divided into two parts.

(i) When $0 \le t \le t_0$, $c(t) = nt$, the direct integration of Eq. (10) yields

$$f_1(t)=\big[e_1(t)\big]^{1-q/p}=\big[e_1(0)\big]^{1-q/p}-0.5\alpha n(1-q/p)t^2. \tag{11}$$

$t_0 > 0$ is the switching time and will be defined later.

(ii) When $t_0 < t$, $c(t) = nt_0$, the direct integration of Eq. (10) results in

$$f_2(t) = \left[e_1(t)\right]^{1-q/p} = \left[e_1(0)\right]^{1-q/p} + 0.5\alpha n(1-q/p)t_0^2 - \alpha n t_0(1-q/p)t. \tag{12}$$

According to Eq. (12), it is found that $[e_1(t_f)]^{1-q/p} = 0$ at the finite time $t = t_f$ defined by

$$t_f(n, t_0) = \left[e_1(0)\right]^{1-q/p} / \left[\alpha n t_0(1-q/p)\right] + 0.5t_0. \tag{13}$$

The total solution of $[e_1(t)]^{1-q/p}$ is summarized as

$$\left[e_1(t)\right]^{1-q/p} = \begin{cases} f_1(t), & 0 \le t \le t_0 \\ f_2(t), & t_0 < t \le t_f \\ 0. & t > t_f \end{cases} \tag{14}$$

From Eq. (14), it is concluded that the error state $e_1(t)$ becomes and remains at zero after the finite time $t = t_f$. That is, $e_1(t_f) = 0$ at $t = t_f$ and $e_1(t) = 0$, $t > t_f$. Additionally, the error state $e_2(t)$ is also converges and remains zero by Eq. (9). This means that $e_2(t_f) = 0$ at $t = t_f$ and $e_2(t) = 0$ at $t > t_f$.

After $t = t_f$, the differential equation of $e_3(t)$ from Eq. (4) simply becomes

$$\dot{e}_3(t) = -(8+h)e_3(t)/3, t > t_f. \tag{15}$$

Then,

$$e_3(t) = e_3(t_f)\exp(-\beta t), t > t_f \tag{16}$$

is further obtained, where $\beta = (8 + h)/3 > 0$. Moreover, $e_3(t)$ satisfies the exponent stability. That is, $e_3(t)$ approaches zero exponentially. Thus, the stability of the error states, $e_1(t)$, $e_2(t)$, and $e_3(t)$, is proven completely.

(2) The finite time $t = t_f$ in Eq. (8) and the switching time $t_0 > 0$ are addressed as follows. Because the control input is bounded $|\mu(t)| \le u_{\max}$, the following result is provided by Eqs. (7) and (9):

$$\begin{aligned} &\left|\dot{c}(t)\left[e_1(t)\right]^{q/p} + c(t)(\alpha q/p)\left[e_2(t) - e_1(t)\right]\left[e_1(t)\right]^{(q/p)-1}\right| \le u_{max} - M \\ &\Rightarrow \left|\dot{c}(t)\left[e_1(t)\right]^{q/p} + c^2(t)(\alpha q/p)\left[e_1(t)\right]^{(2q/p)-1}\right| \le u_{max} - M. \end{aligned} \tag{17}$$

On the basis of the definition of the time function $c(t)$ presented in Eq. (6), the subsequent discussion is divided into two parts.

(i) When $t_0 < t \le t_f$, $c(t) = nt$,

$$\left| n\left[e_1(t)\right]^{q/p} + (nt)^2(\alpha q/p)(nt)^2\left[e_1(t)\right]^{(2q/p)-1} \right| \le u_{max} - M \Rightarrow n\left|e_1(t)\right|^{q/p} \le u_{max} - M.$$

From the fact that the representative point moves towards the demand state on the sliding surface, that is, $|e_1(t)| \le |e_1(0)|$, it is concluded that

$$n \le (u_{max} - M) / \left|e_1(0)\right|^{q/p}. \tag{18}$$

(ii) When $t > t_0$, $c(t) = nt_0$, Eq. (17) yields

$$\left| (\alpha q / p)(nt_0)^2\left[e_1(t)\right]^{(2q/p)-1} \right| \le u_{max} - M \Rightarrow t_0 \le \frac{\sqrt{p(u_{max} - M)/(\alpha q)}}{n\sqrt{\left|e_1(0)\right|^{(2q/p)-1}}}. \tag{19}$$

According to Eq. (13), it is obvious that $\partial t_f / \partial n < 0$. The final time $t_f(n, t_0)$ can take a minimal value only on the boundary of the variable n domain. That is,

$$n = (u_{max} - M) / \left|e_1(0)\right|^{q/p}. \tag{20}$$

The switching time at $t_0 > 0$ is obtained from Eqs. (19) and (20) as

$$t_0 = \sqrt{\frac{\left|e_1(0)\right|}{(\alpha q / p)(u_{max} - M)}}. \tag{21}$$

The minimal value of the final time is yielded by substituting Eqs. (20) and (21) into Eq. (13); the finite time $t = t_f$ is proven as

$$t_f = \left(\frac{1}{1 - (q/p)} \sqrt{\frac{q}{\alpha p}} + \frac{1}{2} \sqrt{\frac{p}{\alpha q}} \right) \sqrt{\frac{\left|e_1(0)\right|}{u_{max} - M}}. \tag{22}$$

This completes the proof of Theorem 2.

The control law presented in Theorem 1 suffers from a pronounced chattering issue in the control input signal, which is evident in the numerical simulation outcomes. To address this chattering behavior, an adaptive control strategy incorporating the time-varying sliding mode function in Eq. (5) is developed in the subsequent section.

Theorem 3.

The control input $\mu(t)$ in Eq. (2) is introduced as

$$\begin{aligned}\mu(t) = &-\dot{c}(t)\left[e_1(t)\right]^{q/p} - c(t)(\alpha q / p)\left[e_2(t) - e_1(t)\right]\left[e_1(t)\right]^{(q/p)-1} \\ &-\left[K_0(t) + K_1(t)\left|e_1(t)\right| + K_2(t)\left|e_2(t)\right|\right]\operatorname{sign}(\sigma(t)),\end{aligned} \tag{23}$$

where sign(·) denotes the sign function. $K_0(t)$, $K_1(t)$, and $K_2(t)$ are the adaptive feedback gains updated according to the following adaptation algorithms:

$$\dot{K}_0(t) = \gamma_0\left|\sigma(t)\right|, \quad K_0(0) = 0, \quad \gamma_0 > 0 \tag{24}$$

$$\dot{K}_1(t) = \gamma_1\left|\sigma(t)\right|\left|e_1(t)\right|, \quad K_1(0) = 0, \quad \gamma_1 > 0 \tag{25}$$

$$\dot{K}_2(t) = \gamma_2\left|\sigma(t)\right|\left|e_2(t)\right|, \quad K_2(0) = 0, \quad \gamma_2 > 0 \tag{26}$$

where γ_0, γ_1, and γ_2 are the positive constant gains determining the adaptation process. Then, the states of the error dynamical system (4) will asymptotically approach and stay on the sliding surface $\sigma(t) = 0$ defined by Eq. (5).

Proof.

To establish the effectiveness of the control strategy described by Eq. (23), it is sufficient to show that it guarantees the asymptotic convergence of the time-varying sliding mode function to the sliding surface and maintains it there thereafter. In this case, the scale Lyapunov function is selected as

$$\Psi_2(t) = 0.5\sigma^2(t) + 0.5\sum_{i=0}^{2}(K_i(t) - K_i^*)^2 / \gamma_i \geq 0, \tag{27}$$

where $K_i^*, i = 0,1,2$ are positive constants that satisfy the following inequalities:

$$K_0^* > \left|\delta(t) + \Delta f(t) + \Delta(t)\right| > 0, \;\; K_1^* > \left|18 - 60h\right| > 0, \;\; K_2^* > \left|9 + 54h\right| > 0. \tag{28}$$

Taking the time derivative of the function $\Psi_2(t)$ along with the solutions of the error-state dynamical system in Eq. (4), the selection of the time-varying sliding mode function in Eq. (5), and the control input in Eq. (23) associated with Eqs. (24) to (26) yields

$$\begin{aligned}\dot{\Psi}_2(t) &= \sigma\dot{\sigma} + \sum_{i=0}^{2}(K_i - K_i^*)\dot{K}_i / \gamma_i \\ &= \sigma\left[\delta_1 + \delta_2 + \Delta - \left[K_0 + K_1\left|e_1\right| + K_2\left|e_2\right|\right]\operatorname{sign}(\sigma)\right] + \sum_{i=0}^{2}(K_i - K_i^*)\dot{K}_i / \gamma_i \\ &\leq \left|\delta_1 + \delta_2 + \Delta\right|\left|\sigma\right| + \left|18 - 60h\right|\left|\sigma\right|\left|e_1\right| + \left|9 + 54h\right|\left|\sigma\right|\left|e_2\right| - \left[K_0^* + K_1^*\left|e_1\right| + K_2^*\left|e_2\right|\right]\left|\sigma\right| \\ &= -\left(K_0^* - \left|\delta_1 + \delta_2 + \Delta\right|\right)\left|\sigma\right| - \left(K_1^* - \left|18 - 60h\right|\right)\left|\sigma\right|\left|e_1\right| - \left(K_2^* - \left|9 + 54h\right|\right)\left|\sigma\right|\left|e_2\right| < 0.\end{aligned}$$

The condition of $\dot{\Psi}_2(t) < 0$ is satisfied. The time-varying sliding mode function $\sigma(t)$ can asymptotically reach $\sigma(t) = 0$ and stay at $\sigma(t) = 0$. Furthermore, the adaptive feedback gains $K_i(t), i = 0,1,2$ approach the constants $K_i^* > 0, i = 0,1,2$. This completes the proof of Theorem 3.

4. Numerical Studies and Discussion

To assess the effectiveness of the suggested time-varying SMC and adaptive-type control procedures for two identical unified chaotic systems, numerical simulations are performed. With a fixed time-step size of 10^{-6}, the system dynamics are integrated using the fourth-order Runge–Kutta method.

The system parameter $h = 0.6$ for the unified chaotic systems in Eqs. (1) and (2) is chosen. The initial conditions for the master and slave systems are selected as $x_m(0) = 1.5$, $y_m(0) = -2.5$, $z_m(0) = 0.5$ and $x_s(0) = -1$, $y_s(0) = -1$, $z_s(0) = -1$, respectively. To illustrate the resilience of the suggested control systems, in the following numerical studies, we assume that the external disturbance is $\Delta f(t) = \sin(t)$ and the system uncertainty is $\Delta(t) = \cos\sqrt{x_s^2(t) + y_s^2(t) + z_s^2(t)}$. The aforementioned rule states that the positive constants are selected as $M = 25$, $u_{\max} = 27$, $p = 11$, $q = 7$, $\gamma_0 = 0.08$, and $\gamma_1 = \gamma_2 = 0.075$, for the time-varying SMC (7) and the adaptive-type control (23) connected to Eqs. (24) to (26).

Figure 4 shows the time responses for the error states, $e_1(t)$, $e_2(t)$, and $e_3(t)$, of the system of Eq. (4) using the time-varying SMC scheme in Eq. (7). It is demonstrated that state synchronization can be accomplished quickly. The state trajectories are shown in three planes [$e_1(t)$, $e_2(t)$, and $e_3(t)$] in Fig. 5. It is demonstrated that $e_3(t)$ is exponentially stabilized once $e_1(t)$ and $e_2(t)$ converge simultaneously to the settling point (original point).

Figure 6 shows the time responses of the applied control input $\mu(t)$, the time-varying function $c(t)$, and the sliding mode function $\sigma(t)$ using the control strategy of Eq. (7). When the state

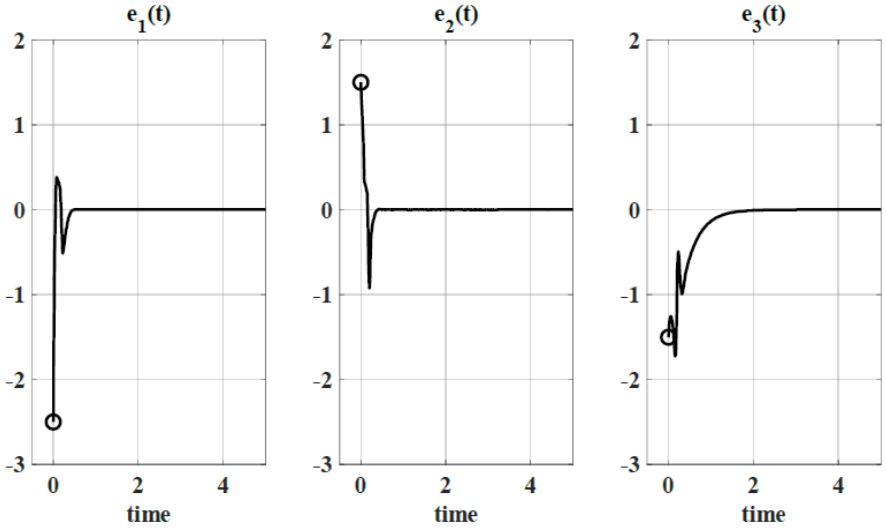

Fig. 4. Time responses for error states by applying control scheme of Eq. (7).

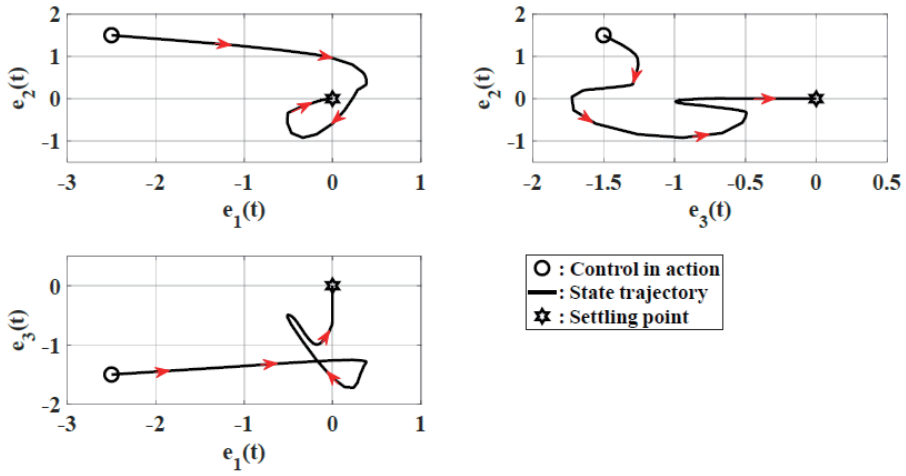

Fig. 5. (Color online) State trajectories by applying control scheme of Eq. (7).

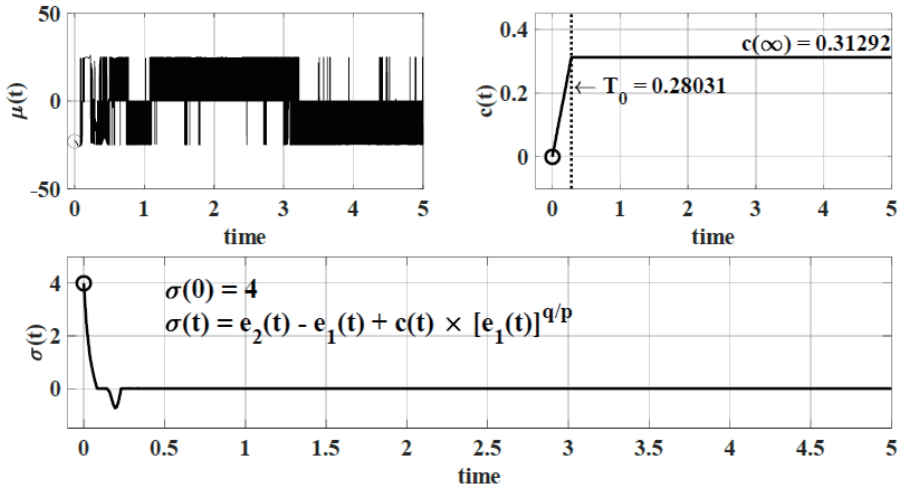

Fig. 6. Time responses of $\mu(t)$, $c(t)$, and $\sigma(t)$ by applying control scheme of Eq. (7).

synchronization control procedure is finished, the time-varying function $c(t)$ is seen to climb linearly from zero until it reaches a constant value, represented as $c(\infty) = 0.3129$, at around $t_0 = 0.28$. Also, the sliding mode function $\sigma(t)$ rapidly approaches zero. Nonetheless, the control input signal $\mu(t)$ has a clearly significant chattering impact. Thus, Eqs. (23) to (26) present an adaptive-type time-varying SMC technique to overcome the chattering effect of $\mu(t)$.

Figure 7 shows the time responses for the error states of system (4) on applying the adaptive control technique described by Eqs. (23) to (26). After $t = 4.335$, it is demonstrated that the error states, $e_1(t)$, $e_2(t)$, and $e_3(t)$, have converged to zero, indicating that the state synchronization is complete. The time response of the applied control input $\mu(t)$ and the sliding mode function $\sigma(t)$ are displayed in Fig. 8. It is demonstrated that the sliding mode function $\sigma(t)$ is stabilized and that the chattering effect of the control input $\mu(t)$ is enhanced.

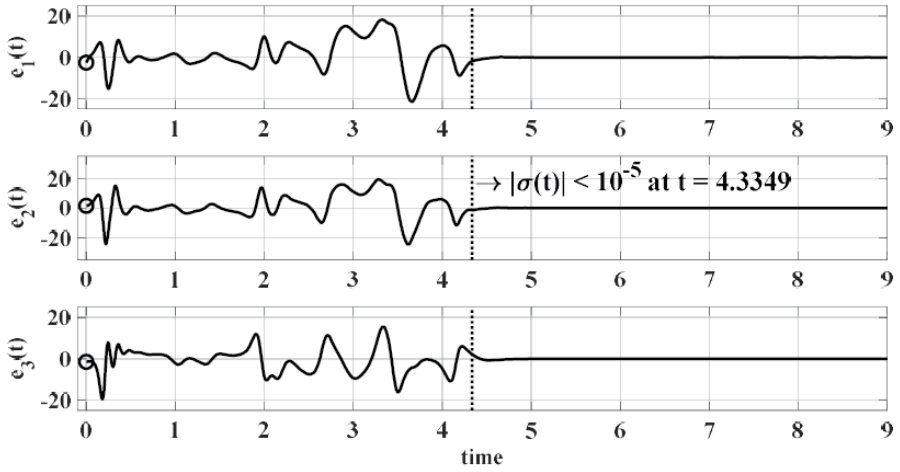

Fig. 7. Time responses for error states by applying control scheme of Eq. (23).

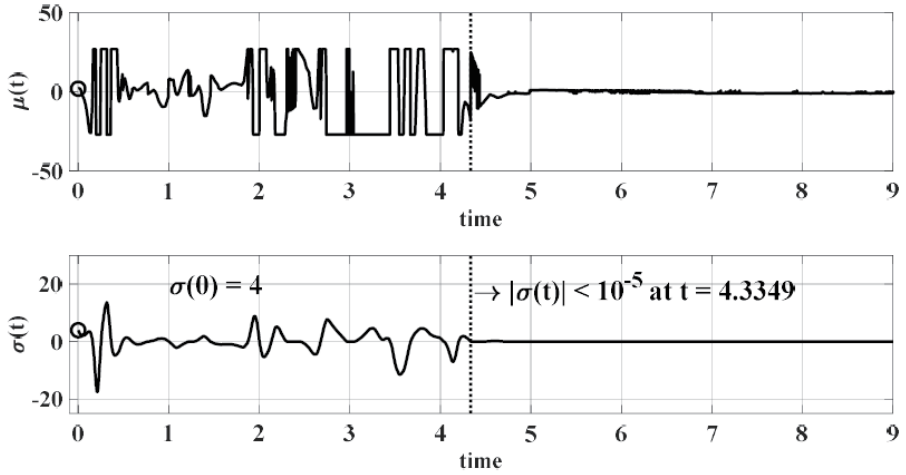

Fig. 8. Time responses $\mu(t)$ and $\sigma(t)$ by applying control scheme of Eq. (23).

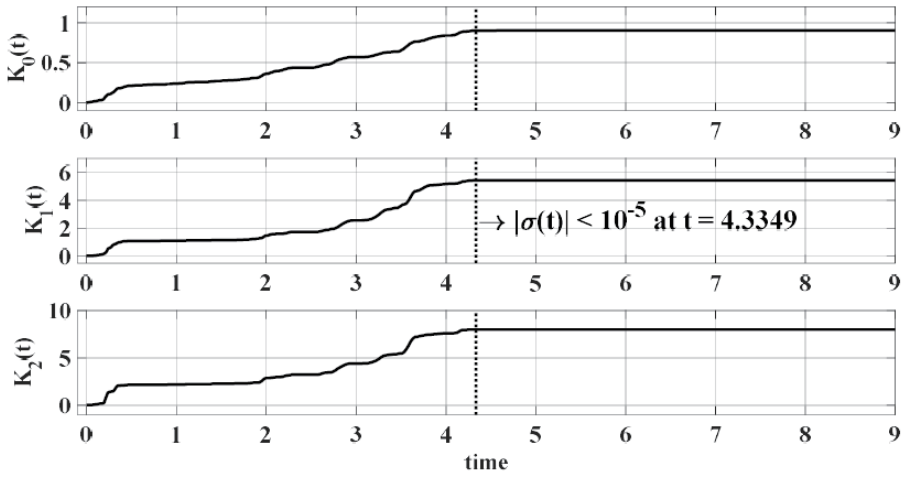

Fig. 9. Time responses of the adaptive feedback gains $K_i(t)$, $i = 0,1,2,3$.

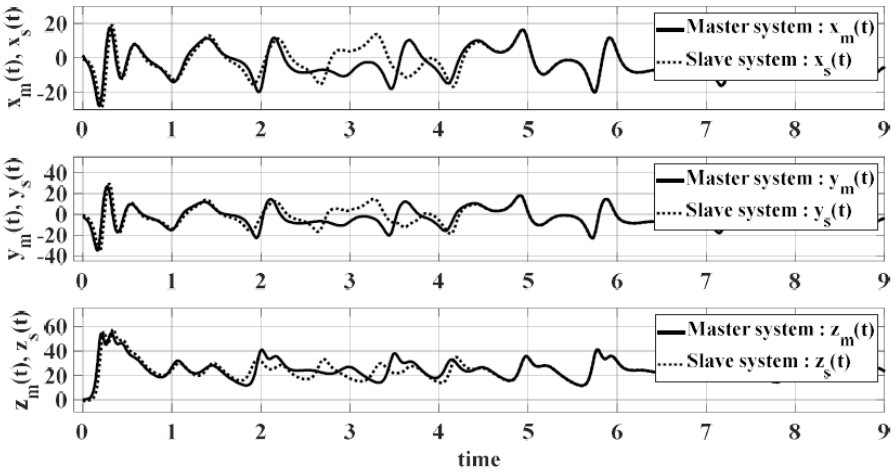

Fig. 10. Time responses of states for the master and slave unified chaotic systems.

The time response of the adaptive feedback gains $K_i(t)$, i = 0,1,2,3 is displayed in Fig. 9. In the presence of lumped system uncertainties and external disturbances, it is demonstrated that the time-varying gains $K_i(t)$, i = 0,1,2,3 attain the steady state after the state synchronization is complete. The respective temporal responses of systems (1) and (2) are shown in Fig. 10. The achievement of state synchronization is clearly demonstrated.

5. Conclusions

The time-varying SMC strategy with an adaptive mechanism for the state synchronization of two unified chaotic systems is addressed in the study. A time-varying sliding mode function and the control law are first designed to drive and maintain error states on the sliding surface. Complete state synchronization is achieved with two error states converging in finite time and the third decaying exponentially. Moreover, the adaptive time-varying SMC scheme is introduced to reduce the chattering effect of control input by using online-updated feedback gains without prior knowledge of system uncertainties. Stability is proven via Lyapunov theory, and simulations confirm the scheme's effectiveness and robustness. Furthermore, the proposed control algorithm, designed to advance state synchronization in unified chaotic systems, holds promise for applications in secure signal transmission and sensing. The pending problems lie in developing a detailed chaotic-synchronization-based ACSK system incorporating the proposed algorithm and facing limitations such as the degradation of the designed system's noise mitigation efficacy and the expenses of hardware implementation for nonlinear control logic. Overcoming these hurdles is a future topic of this study.

Acknowledgments

The author acknowledges the support from the School of Intelligent Manufacture and Electronic Engineering, Guangzhou Institute of Science and Technology.

References

1 Y. Feng, Z. Wei, UL. E. Kocamaz, A. Akgül, and I. Moroz: Complexity **2017** (2017) 7101927. https://doi.org/10.1155/2017/7101927
2 S. Zhu, Q. Lu, Y. Feng, and D. Yan: IEEE Access **12** (2024) 145483. https://doi.org/10.1109/ACCESS.2024.3472123
3 H. Tian, X. Yi, Y. Zhang, Z. Wang, X. Xi, and J. Liu: Symmetry **17** (2025) 1252. https://doi.org/10.3390/sym17081252
4 C. J. A. Luo and F. Y. Wang: Commun. Nonlinear Sci. Numer. Simul. **7** (2002) 31. https://doi.org/10.1016/S1007-5704(02)00005-9
5 Z.M. Ge, T.C. Yu, and Y.S. Chen: J. Sound Vib. **268** (2003) 731. https://doi.org/10.1016/S0022-460X(02)01607-3
6 X. Wu, Z. Gui, Q. Lin, and J. Cai: Nonlinear Dyn. **59** (2010) 427. https://doi.org/10.1007/s11071-009-9549-1
7 S. Lia, Q. Lib, J. Lia, and J. Feng: Nonlinear Anal. Real World Appl. **12** (2011) 1950. https://doi.org/10.1016/j.nonrwa.2010.12.011
8 E. D. S. Oliveira and U. Nackenhorst: Probab. Eng. Mech. **75** (2024) 103556. https://doi.org/10.1016/j.probengmech.2023.103556
9 E. E. Mahmoud, P. Trikha, L. S. Jahanzaib, and O. A. Almaghrabi: Chaos, Solitons Fractals **141** (2020) 110348. https://doi.org/10.1016/j.chaos.2020.110348
10 B. Zolfaghari and T. Koshiba: Appl. Syst. Innov. **5** (2022), 57. https://doi.org/10.3390/asi5030057
11 L. Stenflo: Phys. Scr. **53** (1996) 83. https://doi.org/10.1088/0031-8949/53/1/015
12 L. M. Pecora and T. L. Carroll: Phys. Rev. Lett. **64** (1990) 821. https://doi.org/10.1103/PhysRevLett.64.821
13 S. Iqba and J. Wang: Phys. Scr. **100** (2025) 025243. https://doi.org/10.1088/1402-4896/ad9cfe
14 Y. Xie, Z. Yang, M. Shi, Q. Zhuge, W. Hu, and L. Yi: Adv. Photonics Nexus **3** (2024) 016003-1. https://doi.org/10.1117/1.APN.3.1.016003
15 Y. Luo, Y. Huang, F. Yu, D. Liangm, and H. Lin: Math. **13** (2025) 128. https://doi.org/10.3390/math13010128
16 C. Y. Lin, S. C. Wu, P. H. Kuo, M. J. Huang, S. W. Hong, and H. T. Yau: IEEE Sens. J. **23** (2023) 11453. https://doi.org/10.1109/JSEN.2023.3265777
17 A. Shumran and A. B. A. Al-Hussein: Iraqi J. Electr. Electron. Eng. **20** (2024) 85. https://doi.org/10.37917/ijeee.20.2.8
18 C. C. Yang: Nonlinear Dyn. **63** (2011) 447. https://doi.org/10.1007/s11071-010-9814-3
19 C. C. Yang: J. Franklin Inst. **349** (2012) 349. https://doi.org/10.1016/j.jfranklin.2011.11.013
20 H. Chaudhary, A. Khan, U. Nigar, S. Kaushik, and M. Sajid: Entropy **24** (2022) 529. https://doi.org/10.3390/e24040529
21 J. Sun, Y. Wang, Y. Wang, and Y. Shen: Nonlinear Dyn. **85** (2016) 1105. https://doi.org/10.1007/s11071-017-3338-z
22 X. Xi, S. Mobayen, H. Ren, and S. Jafari: J. Vib. Control **24** (2018) 3842. https://doi.org/10.1177/1077546317713532
23 T. Nguazon, T. Nguekeng, R. Tchitnga, and A. Fomethe: Adv. Mech. Eng. **11** (2019). https://doi.org/10.1177/1687814018822211
24 J. Sun, Y. Wu, G. Cui, and Y.-F. Wang: Nonlinear Dyn. **88** (2017) 1677. https://doi.org/10.1007/s11071-017-3338-z
25 W. Chen, R. Zhang, L. Zhao, H. Wang, and Z. Wei: Proc. Inst. Mech. Eng. Part J. Automob. Eng. **233** (2019) 776. https://doi.org/10.1177/0954407017753529
26 C. Wang, J. Tang, B. Jiang, and Z. Wu: Math. Biosci. Eng. **19** (2022) 2616. https://doi.org/10.3934/mbe.2022120
27 J. Ni, L. Liu, C. Liu, X. Hu, and T. Shen: Nonlinear Dyn. **86** (2016) 401. https://doi.org/10.1007/s11071-016-2897-8
28 H. Tian, Z. Wang, P. Zhang, M. Chen, and Y. Wang: Complexity **2021** (2021) 8865522. https://doi.org/10.1155/2021/8865522
29 C. C. Yang and C. R. Ou: Commun. Nonlinear Sci. Numer. Simul. **18** (2013) 682. https://doi.org/10.1016/j.cnsns.2012.07.012
30 C. C. Yang: Nonlinear Dyn. **72** (2013) 695. https://doi.org/10.1007/s11071-012-0746-y
31 C. C. Yang and C. L. Lin: J. Vib. Control **21** (2015) 601. https://doi.org/10.1177/1077546313487243
32 M. C. Pai: Int. J. Dyn. Control **7** (2019) 1101. https://doi.org/10.1007/s40435-018-0486-z
33 C. H. Yang, K.C. Wang, L. Wu, and R. Wen: Math. Probl. Eng. **2020** (2020) 5391984. https://doi.org/10.1155/2020/5391984
34 D. Ghosh, M. Frasca, A. Rizzo, S. Majhi, S. Rakshit, K. Alfaro-Bittner, and S. Boccaletti: Phys. Rep. **949** (2022) 1. https://doi.org/10.1016/j.physrep.2021.10.006
35 J. Lü and G. Chen: Int. J. Bifurcation Chaos **12** (2002) 659. https://doi.org/10.1142/S0218127402004620

36 E. N. Lorenz: J. Atmos. Sci. **20** (1963) 130. https://doi.org/10.1175/1520-0469(1963)020<0130:DNF>2.0.CO;2
37 G. Chen and T. Ueta: Int. J. Bifurcation Chaos **9** (1999) 1465. https://doi.org/10.1142/S0218127499001024
38 S. Celikovsky and G. Chen: Chaos, Solitons Fractals **26** (2005) 1271. https://doi.org/10.1016/j.chaos.2005.02.040
39 M.T. Yassen: Chaos, Solitons Fractals **26** (2005) 913. https://doi.org/10.1016/j.chaos.2005.01.047
40 H. Takhi, K. Kemih, L. Moysis, and C. Volos: Math. Comput. Simul. **181** (2021) 150. https://doi.org/10.1016/j.matcom.2020.09.020
41 W. Wei, J. Wang, M. Zuo, and J. Du: Inf. Technol. J. **13** (2014) 1126. https://doi.org/10.3923/itj.2014.1126.1132
42 H. Wang, Z. Han, Q. Xie, and W. Zhang: Commun. Nonlinear Sci. Numer. Simul. **14** (2009) 2239. https://doi.org/10.1016/j.cnsns.2008.04.015
43 A. Kumar, and P. P. Singh: IETE J. Res. **69** (2022) 7141. https://doi.org/10.1080/03772063.2022.2060873
44 T. Bonny, W. A. Nassan, and A. Baba: Multimed Tools Appl. **82** (2023) 1067. https://doi.org/10.1007/s11042-022-13317-w
45 N. Tihomorskis, A. Ahrens, and A. Aboltins: Chaos **6** (2024) 170. https://doi.org/10.51537/chaos.1424487